Journal of Applied Electrochemistry (2006) 36:813–819
DOI 10.1007/s10800-006-9140-0

Evaluation of concepts for hydrogen – chlorine fuel cells

MAGNUS THOMASSEN[1,*], ESPEN SANDNES[1], BØRRE BØRRESEN[1,2] and REIDAR TUNOLD[1]
[1]*Department of Materials Science and Engineering, Norwegian University of Science and Technology, NO-7491, Trondheim, Norway*
[2]*Current address: Statoil Research Centre, Arkitekt Ebbells vei 10 NO-7005, Trondheim, Norway*
*(*author for correspondence, e-mail: magnus.thomassen@material.ntnu.no)*

Received 7 July 2005; accepted in revised form 2 March 2006

Key words: chlorine, fuel cell, hydrochloric acid, hydrogen, Nafion, PBI

Abstract

Three different concepts for H_2–Cl_2 fuel cells have been evaluated. An ordinary PEM fuel cell based on a Nafion membrane, a fuel cell based on a combination of circulating hydrochloric acid and a Nafion membrane and a system based on a phosphoric acid doped Polybenzimidazole (PBI) membrane. None of the investigated systems were able to demonstrate stable operation under the conditions used in this study, due to electrocatalyst corrosion, membrane dehydration and/or electrode flooding. All systems studied achieved open circuit voltages close to the reversible thermodynamic value for production of aqueous hydrochloric acid, suggesting formation of dissolved HCl in the electrolyte and fast electrode kinetics.

1. Introduction

Fuel cells are in general used as generators for electric energy, either for mobile or stationary applications. The fuel may either be pure hydrogen, a hydrogen rich fuel or a hydrocarbon. The oxidant in all these cases is oxygen, either pure or more commonly from air. In a H_2–Cl_2 fuel cell, the oxidant (O_2) has been substituted by chlorine. Hence the product from such systems is not water, but hydrogen chloride.

The use of H_2–Cl_2 fuel cells has been investigated both for space and ground applications [1–5] due to the faster electrode kinetics for the chlorine reduction compared to oxygen reduction, which implicates a possible higher energy efficiency of systems applying Cl_2 rather than O_2. For reversible energy storage systems, where HCl is split into H_2 and Cl_2 by electrolysis in periods with excess of electric energy and converted to HCl in a fuel cell during periods of demands of electric energy, the overall energy efficiency has been calculated to be about 70% [3, 6]. Corresponding systems applying oxygen as oxidant and water as the reaction medium are commonly operating at an energy efficiency of around 50% [7]. The use of H_2–Cl_2 fuel cells for industrial applications has been proposed for plants having excess of hydrogen and chlorine readily available and where HCl is needed in the process, such as the chlor-alkali industry. Energy savings for such plants obtained by applying this technology has been estimated to be 2% when using 5% of the produced hydrogen and chlorine for production of HCl required for brine acidification [5]. Furthermore, the use of such units in other industries where chlorine is produced, e.g. in magnesium electrowinning, can be beneficial both with respect to economy and environmental considerations. The electrochemical conversion of hydrogen and chlorine to hydrogen chloride rather than by combustion will supply high value electric energy instead of low value heat.

From a constructional point of view, a H_2–Cl_2 fuel cell could use any electrolyte being either proton or chloride conducting. Depending on the electrolyte, the characteristics of the system will vary. The purpose of this work was to study the possibility of developing a H_2–Cl_2 fuel cell system for industrial applications by considering three different cell configurations, and define the characteristics of each of these systems. The three systems were: (a) a conventional PEM fuel cell applying a Nafion membrane, (b) a composite system applying an aqueous HCl electrolyte and Nafion membrane and (c) a phosphoric acid doped PBI membrane fuel cell operating at intermediate temperatures (150–175 °C).

2. Experimental

2.1. *Nafion PEM fuel cell*

A fuel cell with cylindrical graphite current collectors with serpentine flow fields was used. The active electrode area was 5 cm^2. The membrane electrode assemblies (MEA) were constructed using ELAT gas diffusion

electrodes (E-TEK) with a 20 wt% Pt/C catalyst loading of 1 mg Pt cm^{-2} and a Nafion content of 0.8 mg cm^{-2} hot pressed at 130 °C and a pressure of 10 MPa for 3 min onto a Nafion 115 membrane. The mechanical pressure on the MEA after being loaded into the fuel cell housing was controlled by a pneumatic piston and was set to 1 MPa. The gases, hydrogen (5.0 AGA) and chlorine (2.8 Gerling Holtz) were humidified by thermostatically controlled bubble humidifiers. The humidifiers consisted of an inner saturation tank heated by a water filled outer tank, both made of glass. Steady state polarisation curves were recorded using a Bank HP 20–16 potentiostat connected with Hyscan (Bank Electronics) interface. The cell was operated at 60 °C with a humidification temperature of 90 °C.

2.2. *Composite aqueous/Nafion electrolyte*

The composite aqueous system is a further development of the cell examined previously [8] and a conventional Nafion PEM fuel cell. The intention behind the merging of these two technologies was to solve problems with humidification of the Nafion membrane observed in earlier work and to isolate the platinum catalyst at the anode from the corrosive, chlorine rich liquid electrolyte. The addition of a Nafion membrane to the aqueous system also fills the role as a physical separator to prevent mixing of the reactant gases which, for safety reasons, would most probably be required in an industrial system. In earlier work [8] it was found that the platinum catalyst exposed to the aqueous electrolyte, especially that on the cathode, corroded and probably dissolved as hexachloroplatinic acid (H_2PtCl_6). It was therefore decided to use ruthenium oxide as the cathode catalyst for this fuel cell.

Figure 1 shows a schematic illustration of the cell construction. The fuel cell housing consisted of two graphite current collectors with double serpentine flow fields, a carbon paper anode attached to a Nafion 117 membrane, a PPS (polyphenylsulphone) cloth separator, a carbon paper cathode and a silicon gasket. The graphite current collectors included inlets and outlets for the circulating liquid HCl electrolyte. The PPS cloth acts as a spacer between the electrodes making it possible to apply a mechanical pressure to the electrodes and simultaneously supplying space for the circulating electrolyte.

2.2.1. *Cathode preparation*

The cathodes were constructed of ELAT carbon paper (E-TEK) with various amounts of Teflon impregnation (0–60 wt%). Catalyst inks were prepared using commercial unsupported RuO_2 catalyst (Alpha Aesar). The catalyst was mixed with various amounts of Teflon suspension and isopropanol to produce a range of catalysts with different degrees of wet-proofing. The mixture was stirred and ultrasonicated for several hours before application to the cathode carbon paper electrode using an air-brush (Badger), with the carbon electrode placed on a thermal-controlled heating plate. After spraying, the electrode was dried in a forced convection oven at 150 °C for one hour.

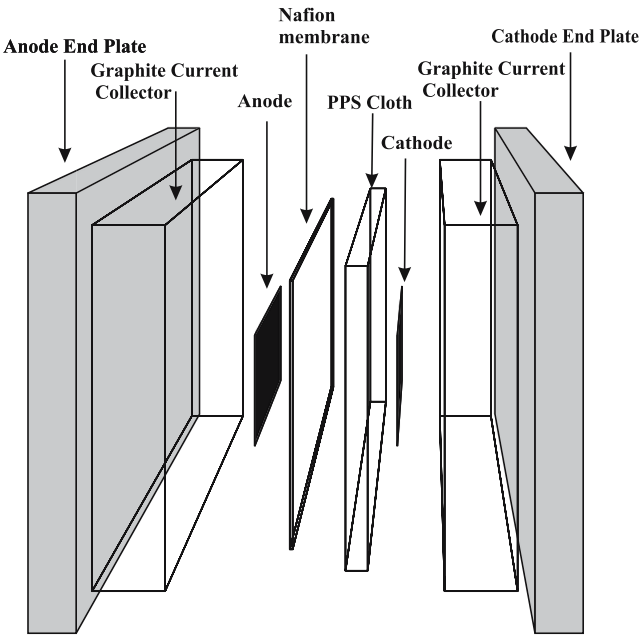

Fig. 1. Schematic illustration of the hybrid fuel cell construction.

2.2.2. *Membrane and MEA preparation*

The Nafion 117 membranes were treated by immersion in 85 °C 18.2 MΩ distilled water for 15 min, thereafter in 5% H_2O_2 (Merck *p.a.*) for 30 min and washed with distilled water and ion exchanged twice in 0.05 M H_2SO_4 (Merck *p.a.*), each time for 30 min. After ion exchange, the membranes were washed thoroughly by immersion in distilled water four times, each for about 15 min. The membranes were then cut in rectangular pieces and stored in purified water. Commercially available ELAT gas diffusion electrodes (E-TEK) with a 20 wt% Pt/C catalyst loading of 1 mg Pt cm^{-2} were used as anodes. A rectangular piece of Nafion membrane was gently dried with a lint free paper, sandwiched with a 6.5 cm^2 rectangular anode piece between two thin Teflon sheets and hot-pressed for 3 min at 130 °C and 10 MPa. The MEA was then cooled and placed in purified water until mounted in the cell.

2.2.3. *Fuel cell testing*

The cell was assembled using a torque of 0.15 N m on the bolts. All experiments reported here were conducted at room temperature and atmospheric pressure. The gases, hydrogen (5.0 AGA) and chlorine (2.8 Gerling Holtz), were fed to the cell with no pre heating or humidification and exited the cell through a water column to create a small overpressure inside the cell (10 cm H_2O). The fuel cell was controlled using a Solartron SI1287 electrochemical interface. Quasi steady-state polarisation curves were recorded at an operating temperature of 25 °C by sweeping the potential at 1 mV s^{-1} from open circuit to approx. 0.2 V and then

reversed. The HCl liquid electrolyte circulated from a thermally controlled external reservoir through the cell at a rate of 2 ml s^{-1} via a peristaltic pump. The HCl electrolyte concentration was varied between 1 and 5 mol dm^{-3}.

2.3. *PBI fuel cell*

2.3.1. *Fuel cell construction and testing*

The MEA consisted of a phosphoric acid doped PBI membrane with attached gas diffusion electrodes. The catalyst loading was 0.4 mg 50 wt% Pt/C cm^{-2} on the anode and 0.6 mg 50 wt% Pt/C cm^{-2} on the cathode. Further details of the experimental cell and MEA preparation can be found in [9]. The MEA was mounted in a graphite fuel cell housing (Electrochem) with an active area of 6.25 cm^2. The housing was fitted with heating elements and the cell temperature was measured by a thermocouple and controlled by a PID regulator. The fuel cell was controlled using a Solartron SI1287 electrochemical interface and quasi steady-state polarisation curves were recorded by sweeping the potential at 1 mV s^{-1} from open circuit to approx. 0.2 V and then reversed to open circuit at temperatures between 125 and 175 °C and atmospheric pressure. Hydrogen (5.0 AGA) and either chlorine (2.8 Gerling Holtz) or oxygen (2.0 AGA) was humidified by passing through bubble flasks with purified water at room temperature.

2.3.2. *Resistance measurements*

The ohmic resistance in a fuel cell may be assessed either by current interrupt techniques or by high frequency impedance measurements [10, 11]. The current interrupt technique is easier to implement and requires less equipment. Current interrupt is based on breaking the electronic circuit and measuring the potential transient of the cell. The cell voltage of a fuel cell consists of various components and may be expressed as:

$$E = E^{\text{rev}} - \sum \eta - IR_{\text{cell}} \tag{1}$$

where $\sum\eta$ is the sum of the overvoltages related to the electrode kinetics, IR is the potential drop due to the ohmic resistance in the electrodes and electrolyte and E^{rev} is the thermodynamical voltage of the cell. Both the overpotentials and the ohmic potential drop are dependent on the current passing in the system. The voltage change at the moment the circuit is broken, ΔE_{inst}, is related to the circuit resistance through Ohm's law:

$$\Delta E_{\text{inst}} = R_{\text{cell}}\Delta I \tag{2}$$

In a real electrochemical cell, the local current in parts of the cell might not drop instantly to zero due to electrochemical processes occuring in the electrodes. In a fuel cell, this will lead to a potential gradient through the porous electrodes and the resistance estimated from Eq. (2) will be too high; that is, some of the polarization overvoltage is erroneously attributed to the ohmic resistance of the cell. The potential relaxation of the porous electrodes is closely connected to the exchange current density, i_0, of the electrochemical reactions and the error in the estimated ohmic resistance increases with decreasing i_0 [11].

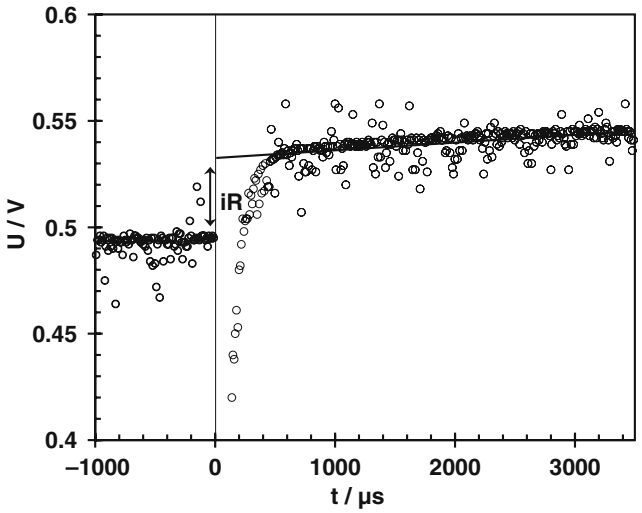

Fig. 2. Typical cell voltage transient after current interruption.

The resistance in the PBI fuel cell was measured using the current-interruption technique. An electrical switch was installed between the counter electrode and the potentiostat and a digital oscilloscope (Pico-technologies) was used to measure the voltage transient from the interruption of the circuit. The cell was run galvanostatically at current densities of approx. 0.2 A cm^{-2} during these measurements. Figure 2 shows a typical voltage transient for the fuel cell at current interruption.

Immediately after the circuit break the voltage signal is noisy, making it impossible to select a representative value for the cell potential. Instead, the voltage change at the current interrupt can be calculated by extrapolating a linear fit to the data recorded some time after the interruption back to $t = 0$ as shown in Figure 2.

The cell was fed with oxygen and operated galvanostatically until a stable potential and resistance was obtained. The feed was then changed to chlorine gas ($t = 0$) and several consecutive current interruption measurements were performed until relatively stable values of the cell voltage and resistance were observed.

3. Results and discussion

3.1. *General thermodynamics*

A simple thermodynamic overview of the temperature dependence of the open circuit voltage of the hydrogen–chlorine fuel cell is presented in Figure 3. Thermodynamic data for the reactants and products at 25 °C [12] have been used to calculate the cell voltage dependency for an aqueous and gaseous reaction respectively.

$$1/2\ H_{2(aq)} + 1/2\ Cl_{2(aq)} \rightleftharpoons HCl_{(aq)} \tag{3}$$

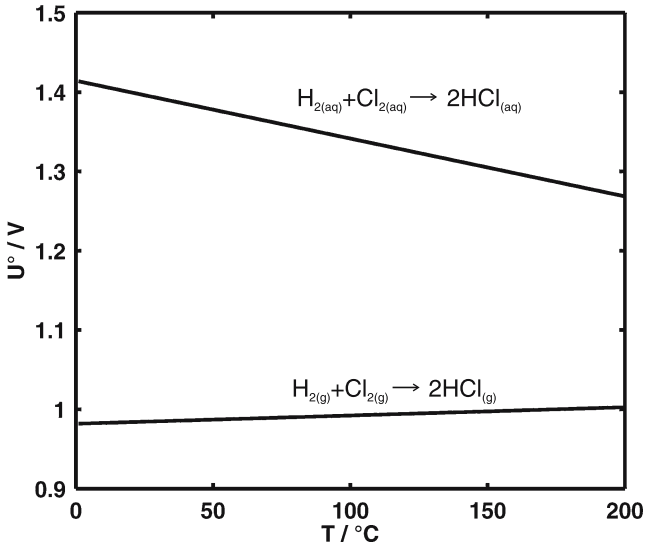

Fig. 3. Temperature dependence of the thermodynamic cell voltages of the hydrogen–chlorine fuel cell with an aqueous or gaseous phase reaction.

$$1/2\ H_{2(g)} + 1/2\ Cl_{2(g)} \rightleftharpoons HCl_{(g)} \qquad (4)$$

It is clearly seen that due to the strong exothermic energy associated with dissolution of hydrogen chloride in water, the theoretical cell voltage will be strongly dependent on the system in question. For a system where the product is an aqueous solution of HCl, the maximum theoretical cell voltage is 1.39 V at 25 °C at standard conditions, while a gaseous reaction would only yield cell voltage of 0.98 V. It is also interesting that the voltage of the aqueous system decreases with increasing temperature, while the gaseous system displays a slight increase in cell voltage. This rather unexpected behaviour of the gaseous system is due to the negative entropy term in this reaction.

3.2. *Nafion PEM fuel cell*

The results of steady state polarisation of the Nafion fuel cell using oxygen and chlorine as cathode feed are given in Figure 4. The cells are operated at 60 °C and with gas humidification of both anode and cathode gases.

The open circuit voltage is drastically increased (from 0.9 V to 1.35 V) when switching from oxygen to chlorine as oxidant. However, the maximum electrical power output is not increased. The data points from the polarisation of the chlorine fed cell show a much larger scatter than for the oxygen fuel cell as the current output at a given potential constantly decreases with time. This demonstrates the unstable behaviour of the system compared to the oxygen fuelled cell. It is also clearly seen that the resistance of the cell fed with chlorine is much higher than that of the oxygen cell, as the slope of the Cl_2 polarisation curve is much steeper than that for

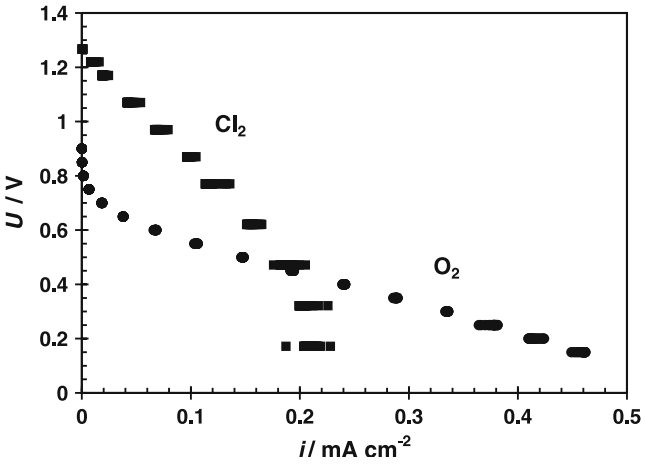

Fig. 4. Polarisation curves obtained from Nafion fuel cell operated on oxygen and chlorine at 60 °C.

oxygen. This indication of a membrane conductivity decrease was further investigated by electrochemical impedance spectroscopy at various potentials. This showed values for the cell resistance of 0.35 Ω for the oxygen cell and a value of 0.5–1.0 Ω for the chlorine fed cell. This increase in cell resistance is most probably due to the removal of water in the membrane by the hydrochloric acid produced. A reduction in water content in the Nafion membrane will drastically reduce the proton conductivity and thus yield a higher ohmic resistance in the cell [13]. A reduction in electrolyte conductivity will also influence the potential and current distribution in the porous electrodes so that the utilisation of the available electrocatalyst is reduced.

From Figure 4 it can be seen that the overpotential for oxygen reduction is in the order of 400 mV before any appreciable current is supplied by the cell. For the cell fuelled with chlorine however, a significant amount of current is produced after a polarisation of 50 mV. This strongly indicates that the kinetics of the chlorine reduction reaction is much better than the kinetics for oxygen reduction.

3.3. *Composite aqueous/Nafion electrolyte*

A typical steady state polarisation curve of the fuel cell with an electrolyte consisting of both a liquid circulating electrolyte and a Nafion membrane is shown in Figure 5. It can be observed from the linear current/potential curve at low currents that the open circuit potential is close to the thermodynamical value and that the activation overpotential appears to be small. A mass transport controlled behaviour is apparent at current densities above 0.3 A cm^{-2}.

Under operation, leakage of electrolyte through the electrodes and into the gas channels was a constant problem, especially on the cathode side. Intrusion of chlorine gas into the electrolyte was also frequently observed. Multiple electrodes with varying amounts of Teflon impregnation, both in the gas diffusion layer and

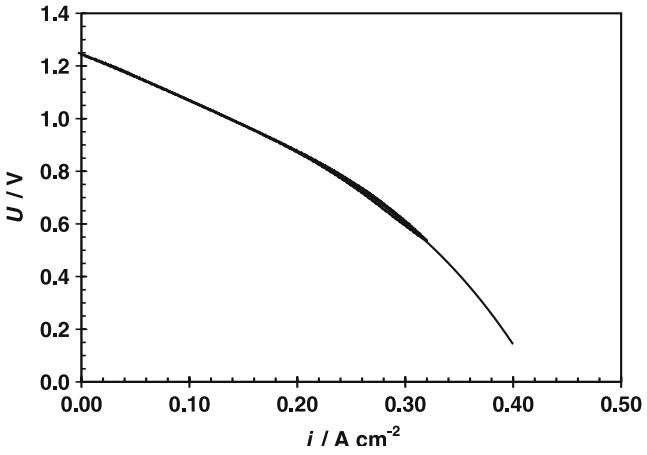

Fig. 5. Polarisation curves obtained from the composite fuel cell operated on 3 mol dm^{-3} HCl and an operating temperature of 25 °C.

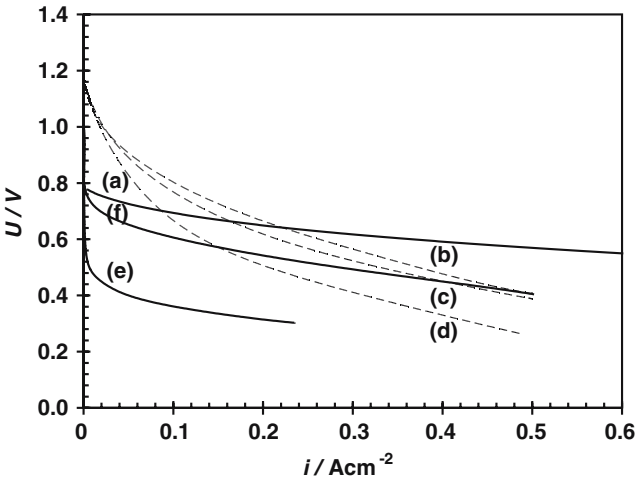

Fig. 6. Polarisation curves obtained from PBI fuel cell operated at 175 °C on oxygen and chlorine. Curve a is the original polarisation curve of the cell fed with O_2 and H_2, curves b, c and d are polarisations (in chronological order) while the cell is fed with Cl_2. Curves e and f are cell polarisations with O_2 after Cl_2 operation.

the catalyst layer, was tested and a reduction of leakage was observed with high degrees of electrode wet proofing. However, no significant difference in the performance or operating stability of the fuel cell was established. In addition to an irregular cell performance, the reproducibility between identical electrodes was poor.

The high open circuit voltage of this fuel cell indicates that the majority of the produced HCl is dissolved in the aqueous phase. At standard conditions, the thermodynamical potential of the chlorine electrode is 1.36 V for formation of aqueous HCl compared to 0.98 V for gaseous HCl. In this system, with an aqueous electrolyte in which the formed HCl is dissolved, the liquid phase has to be circulated to remove the product from the cell. A gradual increase in HCl concentration in the electrolyte itself would unavoidably cause an unevenness of the current distribution along the electrode and/or through the stack due to a change in the reversible voltage of the system. A more detailed analysis of these effects is performed in [14].

3.4. *PBI fuel cell*

3.4.1. *Polarization curves*

Figure 6 shows polarisation curves for the PBI fuel cell running on oxygen (full lines) and chlorine (dashed lines) at 175 °C. There is a significant difference in the open circuit cell voltage when operating on oxygen or chlorine. The OCP of the oxygen-fed cell lies several hundred millivolts below the thermodynamic value, while for chlorine the theoretical and actual cell voltage are nearly identical. The different lines were recorded in chronological order, from (a) to (f). The first polarisation (a) was performed using oxygen as feed. The feed was then changed to chlorine and curves (b) to (d) was recorded successively. The feed was then changed back to oxygen and curves (e) and (f) was recorded with an hour of operation at 0.4 V between the curves.

The open circuit voltage of the cell when operated on chlorine is 1.15 V, which is close the thermodynamic potential for formation of aqueous HCl. This indicates that the produced HCl is formed as a dissolved species in the immobilized phosphoric acid in the polymer matrix and not directly as gaseous HCl. Based on the high open circuit voltage it can be assumed that the kinetics for the reduction of chlorine is also rapid in this system. The three curves b, c and d were as previously stated, recorded in chronological order and it is clearly seen that the performance of the fuel cell decreases rapidly with time. This decrease may be attributed to either catalyst degradation, reduction of the ionic conductivity of the polymer electrolyte or a combination of these. The cell was then switched to an oxygen feed and a polarization curve was recorded (curve e). The resulting performance was poor. However, a slight increase in performance was observed during the recording of the polarisation curve and after running the cell at 0.4 V for approximately one hour another polarisation curve was recorded (curve f). The curve shows that performance had improved drastically and approached that prior to exposing it to chlorine.

3.4.2. *Resistance measurements*

To further elucidate the cause of the reduction in cell performance when feeding the cell with chlorine, current interruption measurements were performed on the cell while changing the feed from oxygen to chlorine. The current-interrupt resistance measurements of the PBI fuel cell can be seen in Figure 7. The open circles represent the cell resistance (R_{cell}) and voltage (U_c), while the open squares are the calculated iR-free cell voltage. When fed with oxygen, the value of the cell resistance was found to be close to 0.2 Ω cm^{-2}. Switching to a chlorine feed, the cell resistance increased rapidly reaching values close to 0.5 Ω cm^{-2} within

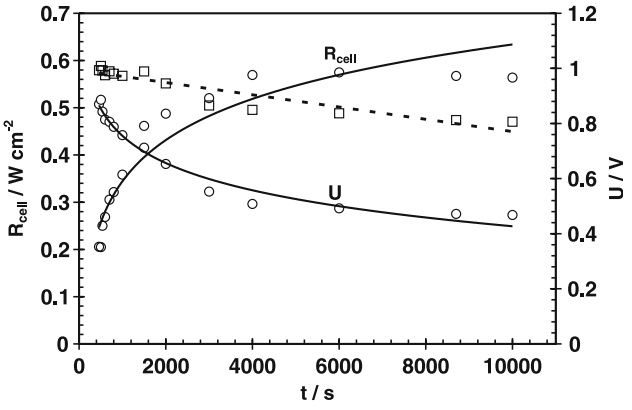

Fig. 7. Current interrupt measurements of PBI fuel cell switched from oxygen to chlorine feed, galvanostatic operation 0.2 A cm^{-2}. Circles and full lines represent the cell voltage and cell resistance, the open squares and dashed line are the iR-corrected cell voltage.

30 min of operation. The resistance further increased to a stable value of 0.55 Ω cm^{-2} during the next 2 h. The full lines in Figure 7 represent a logarithmic increase/decline of the cell resistance and voltage respectively, while the dashed curve represent a linear decrease in the iR-corrected cell voltage.

The drastic increase in cell resistance occuring almost instantaneously after changing to chlorine shows that it is most probably a decrease in the conductivity of the polymer electrolyte that causes the reduction in cell performance and not a degradation of the catalyst. HCl is hygroscopic. Most probably, the production of HCl in the fuel cell causes removal of water from the system and forces the phosphoric acid in the membrane to polymerize to pyrophosphoric acid or higher oligomers [15, 16].

$$H_3PO_4 \rightarrow H_4P_2O_7 \rightarrow H-(HPO_3)_n-OH \qquad (5)$$

This polymerization reaction reduces the proton transport ability of the electrolyte and thus increases the resistance of the cell. It is also possible that the formed HCl replaces the phosphoric acid in the membrane, the conductivity of HCl-doped PBI being at least 10 times lower than PBI doped with phosphoric acid [17]. However, since the performance increased on reverting to oxygen (Figure 6) with the consequential production of water inside the polymer electrolyte, it is more probable that the polymerization of phosphoric acid is the cause of the increased cell resistance.

If an increase in ohmic resistance in the membrane is the only effect of dehydration of the membrane, an iR-corrected cell voltage should be constant with time. From Figure 6 it can be seen that the iR-corrected cell voltage shows a linear decrease with time; thus a simple increase of the membrane resistance cannot fully explain the reduction in performance. A fuel cell electrode has a porous, three dimensional structure consisting of polymer electrolyte, gas pores and a electronically conductive phase. Considering this, an increase in resistance of the polymer electrolyte will decrease the effective utilization of the catalyst particles furthest away from the membrane. This is effectively the same as decreasing the active catalytic area and will have an additional negative effect on cell performance. It is therefore not necessarily corrosion of the platinum catalyst occuring in this system.

To investigate the possibility of platinum catalyst degradation, an oxide catalyst, expected to be more stable, was tested. An MEA with a cathode containing 2 mg cm^{-2} IrO_2 as electrocatalyst was prepared using the same procedure as described in section 1. However, the cell showed similar behaviour with loss of performance and an increase in resistance. Thus, a rapid degradation of the cathode platinum electrocatalyst can be considered to be unlikely. The long term catalyst stability however, might be poor. The degree of gas humidification was also increased to see if this could counteract the resistance increase. The bubble flask was immersed in a temperature controlled water bath and the cell was run at a constant potential of 0.6 V. No appreciable change in cell performance was observed on increasing the bath temperature from room temperature up to 80 °C

A possible solution to the problem of water removal and the subsequent conductivity decrease of the PBI membrane might be to include a certain amount of oxygen bleed into the chlorine flow. This addition of oxygen would, at low enough cell voltages, lead to production of water inside the membrane and possibly retard the polymerisation of phosphoric acid.

3.5. *Comparison of the fuel cell systems*

The systems studied possess different properties which are more or less advantageous. All have a rather high open circuit voltage compared to ordinary hydrogen–oxygen fuel cells and the chlorine electrode kinetics are far better than for the oxygen electrode. Both of these properties lay a good foundation for a fuel cell system with high power density and energy efficiency. However, all the systems studied suffer from severe stability problems.

The main issue for the two cell designs with a solid polymer electrolyte seems to be the highly hygroscopic nature of HCl. Both systems need a certain amount of water to maintain an appreciable electrolyte conductivity and with the production of large amounts of HCl, essentially all water is removed from the system. Even with a high degree of humidification in the Nafion system it was not possible to obtain proper water management, neither was the low amount of water needed in the PBI system [15, 18] able to remain in the electrolyte.

The composite system was designed to avoid the humidification problem observed in the Nafion system and seemed to fulfill this task. However, the inclusion of the liquid electrolyte dramatically increases the corrosivity of the system since it consists of a highly acidic aqueous solution with large amounts of aggressive

chloride anions and dissolved oxidative chlorine. The liquid HCl electrolyte has a low viscosity and the surface tension of HCl solutions is lower than that of water [19]. These physical properties make it extremely hard to contain the electrolyte and place stringent design conditions on the cell housing, gas diffusion electrodes and auxiliary equipment.

4. Conclusions

Three low temperature fuel cell designs were evaluated for use as a hydrogen–chlorine fuel cell for co-production of hydrochloric acid and electric power. It was found that the chlorine reduction kinetics are much faster than the corresponding oxygen reduction reaction, leading to low activation losses at the fuel cell cathode. However, the nature of the reactant, chlorine, and the product, HCl, places strict demands on the corrosion resistance of the construction materials and drastically increases the difficulties related to water management in the cells. Due to these effects, none of the investigated systems were able to demonstrate stable operation under the conditions used in this study. The PBI cell showed best potential and seems to be the system in which the humidification and corrosion difficulties can most easily be remedied. The first design criteria for such a system should be the minimisation of the existence of liquid water, ideally a hydrogen/chlorine fuel cell system should operate in a totally water free environment and consist of a high temperature proton conductor.

Acknowledgements

The authors acknowledge the Research Council of Norway (NFR) and Norsk Hydro ASA for financial support.

References

1. A. Gelb, US Patent (5 041 197).
2. R.S. Yeo, J. McBreen and S. Srinivasan, *J. Electrochem. Soc.* **126** (1979) C379.
3. R.S. Yeo, J. McBreen, A.C.C. Tseung, S. Srinivasan and J. Mcelroy, *J. Appl. Electrochem.* **10** (1980) 393.
4. E.B. Anderson, E.J. Taylor, G. Wilemski and A. Gelb, *J. Power Sources* **47** (1994) 321.
5. E. Anderson, E.J. Taylor, N.R.K. Vilambi and A. Gelb, *Sep. Sci. Technol.* **5** (1990) 1537.
6. E. Gileadi, S. Srinivasan, F.J. Salazano, C. Braun, A. Beaufrere, S. Gottesfeld, L.J. Nuttall and A.B. Laconti, *J. Power Sources* **2** (1977) 191.
7. K. Ledjeff, F. Mahlendorf, V. Peinecke and A. Heinzel, *Electrochim. Acta* **40** (1995) 315.
8. M. Thomassen, B. Børresen, G. Hagen and R. Tunold, *J. Appl. Electrochem.* **33** (2003) 9.
9. F. Seland, T. Berning, B. Børresen and R. Tunold, *J. Power Sources*, in press. doi: 10.1016/j.jpowsour.2006.01.047.
10. T. Mennola, M. Mikkola, M. Noponen, T. Hottinen and P. Lund, *J. Power Sources* **112** (2002) 261.
11. C. Lagergren, G. Lindbergh and D. Simonsson, *J. Electrochem. Soc.* **142** (1995) 231.
12. G. Aylward and T. Findlay, *SI Chemical Data*, 3rd ed., (John Wiley & Sons, New York, 1994).
13. T.A. Zawodzinski, C. Derouin, S. Radzinski, R.J. Sherman, V.T. Smith, T.E. Springer and S. Gottesfeld, *J. Electrochem. Soc.* **140** (1993) 1041.
14. M. Thomassen, B. Børresen, K. Scott and R. Tunold, *J. Power Sources*, In press. doi: 10.1016/j.jpowsour.2005.07.034.
15. Y.L. Ma, J.S. Wainright, M.H. Litt and R.F. Savinell, *J. Electrochem. Soc.* **151** (2004) A8.
16. J. Cho, J. Blackwell, S.N. Chvakun, M. Litt and Y. wang, *J. Polymer Sci. Part B* **42** (2004) 2576.
17. B. Xing and O. Savadogo, *J. New Mat. Electrochem. Systems* **2** (1999) 95.
18. J.S. Wainright, J.T. Wang, D. Weng, R.F. Savinell and M. Litt, *J. Electrochem. Soc.* **142** (1995) L121.
19. R.C. Weast, *in* R.C. Weast (Ed.), *Handbook of Chemistry and Physics 57th edn* (CRC Press, Ohio, 1976).